Quenching of oscillation by the limiting factor of diffusively coupled oscillators

M. Manoranjani,[1] D. V. Senthilkumar,[2,*] Wei Zou,[3] and V. K. Chandrasekar[1,†]

[1]*Centre for Nonlinear Science & Engineering, School of Electrical & Electronics Engineering, SASTRA Deemed University, Thanjavur-613 401, Tamil Nadu, India*

[2]*School of Physics, Indian Institute of Science Education and Research, Thiruvananthapuram 695551, Kerala, India*

[3]*School of Mathematical Sciences, South China Normal University, Guangzhou 510631, China*

(Received 28 June 2022; revised 9 September 2022; accepted 18 November 2022; published 7 December 2022)

A simple limiting factor in the intrinsic variable of the normal diffusive coupling is known to facilitate the phenomenon of reviving of oscillation [Zou *et al.*, Nat. Commun. **6**, 7709 (2015)], where the limiting factor destabilizes the stable steady states, thereby resulting in the manifestation of the stable oscillatory states. In contrast, in this work we show that the same limiting factor can indeed facilitate the manifestation of the stable steady states by destabilizing the stable oscillatory state. In particular, the limiting factor in the intrinsic variable facilitates the genesis of a nontrivial amplitude death via a saddle-node infinite-period limit (SNIPER) bifurcation and symmetry-breaking oscillation death via a saddle-node bifurcation among the coupled identical oscillators. The limiting factor facilities the onset of symmetric oscillation death among the coupled nonidentical oscillators. It is known that the nontrivial amplitude death state manifests via a subcritical pitchfork bifurcation in general. Nevertheless, here we observe the transition to the nontrivial amplitude death via a SNIPER bifurcation. The in-phase oscillatory state loses its stability via the SNIPER bifurcation, resulting in the manifestation of the nontrivial amplitude death state, whereas the out-of-phase oscillatory state loses its stability via a homoclinic bifurcation, resulting in an unstable oscillatory state. Multistabilities among the various dynamical states are also observed. We have also deduced the evolution equation for the perturbation governing the stability of the observed dynamical states and stability conditions for SNIPER and pitchfork bifurcations. The generic nature of the effect of the limiting factor is also reinforced using two distinct nonlinear oscillators.

DOI: 10.1103/PhysRevE.106.064204

I. INTRODUCTION

Oscillation quenching is a fascinating emerging phenomenon whereby the interaction between oscillatory units ceases their oscillation to exist. Investigations on the cessation of oscillation, several times reported as synchronization to stable steady states, under various coupling configurations have witnessed a considerable research activity in the broad field of nonlinear dynamics and complex systems in the recent literature [1–5]. In general, quenching of oscillation is classified as amplitude death (AD), where a system of coupled oscillators populate a fixed point (homogeneous steady state) [1], and oscillation death (OD), where the coupled oscillators populate different fixed points (heterogeneous steady states) [6]. The phenomenon of oscillation quenching has been extensively studied in view of its applications in diverse fields, and substantial insights have been emerged on these distinct scenarios. Amplitude death and oscillation death has its relevance in population ecology, electrochemical oscillators [7], neural networks [2,8], and oscillations in the atmosphere and oceans [9]. Indeed, recent studies have also shown that AD/OD has a great importance in several areas, including oceanography [9], lasers [10], and neuronal systems [8]. In addition, other types of quenching scenarios, such as partial AD and nontrivial amplitude death (NAD), have also been shown to emerge in coupled oscillators and complex networks. In the partial AD, the oscillation of only a few variables of the coupled oscillators is quenched, whereas the remaining variables retain their sustained oscillatory state. Nontrivial amplitude death is distinctly different from amplitude death. The former refers to the stable nontrivial steady state, while the latter refers to the stable trivial steady state.

In particular, it is known that AD generally onsets via either a saddle-node bifurcation or a Hopf bifurcation, while the NAD state manifests via a subcritical pitchfork bifurcation [11–13]. Further, the heterogeneity in terms of the parameter mismatch is conducive to AD while it is detrimental to NAD. It is also evident from a recent review [12] that much less progress has been made on NAD when compared to the literature on the classical AD, which has also been emphasized in the review article. NAD was demonstrated in two coupled Stuart-Landau oscillators, coupled directly via a diffusive coupling and indirectly via a dynamic common environment [14], in delay coupled networks [15]. Nonlinear couplings often manifest a NAD state due to the genesis of a nontrivial homogeneous steady state [2,8]. Indeed, it was demonstrated that any choice of steady state can be stabilized, resulting in NAD, by engineering the nonlinear couplings suitably [2]. Mean-field coupling was also shown to induce NAD states effectively [11,13].

In contrast, the phenomenon of reviving of oscillation involves revival of oscillation from the above-mentioned dis-

*skumar@iisertvm.ac.in

†chandru25nld@gmail.com

tinct stable steady states, by destabilizing them in their own stable parameter space, and by adopting various coupling strategies but without altering the system dynamics. Revival of oscillation has been achieved by employing gradient coupling [16], processing delay [17], a diffusion self-feedback factor [18], low-pass filters [19], and so on. Among these coupling schemes, limiting the interaction in the normal diffusive coupling by introducing a simple limiting factor has shown to be an efficient technique to revoke the oscillation in a wide variety of quenching scenarios and in a large class of complex systems [18]. Since then, the effect of the simple limiting factor in the normal diffusive coupling on the emergent dynamics has been a subject of interest for many researchers [13,20–22], whose focus is on reviving oscillations under various dynamical transitions and scenarios. In all these studies, the limiting factor has been introduced in the intrinsic variable of the diffusive coupling. In contrast, recently the onset of OD has been shown in a system of two chemomechanical oscillators and in coupled Hindmarsh-Rose systems by introducing the limiting factor in the extrinsic variable along with a repulsive coupling [23]. Initiatively, it is easy to recognize that this is simply the inverse effect of the limiting factor in the intrinsic variable by factoring it out.

In this work, in contrast to the effect of reviving of oscillation by the limiting factor in the intrinsic variable, we show that the latter can indeed also lead to the manifestation of the phenomenon of quenching of oscillation, namely, NAD and symmetry-breaking OD in the coupled identical Stuart-Landau oscillators and symmetric OD in the coupled nonidentical Stuart-Landau oscillators. Specifically, diffusive coupling among the x variables is coupled repulsively to the evolution equation of the dissimilar (conjugate) variables, which breaks the rotational symmetry, along with a simple limiting factor to elucidate our results. The bifurcation transitions are illustrated by depicting the bifurcation diagrams obtained using XPPAUT software [24]. The transition to the NAD state has been observed in the literature so far via a subcritical pitchfork bifurcation in general, as mentioned above. However, here we have identified the transition from in-phase oscillations to NAD via a saddle-node infinite-period limit cycle (SNIPER) bifurcation and the coalescence of the saddle and stable node, resulting in an infinite-period limit-cycle solution, in the coupled identical Stuart-Landau oscillators as a function of the repulsive coupling strength. The out-of-phase oscillatory state loses its stability via a homoclinic bifurcation. Multistability between in-phase (IPS) and out-of-phase (OPS) oscillations, between NAD and OPS, and that between OPS and symmetry-breaking OD are also observed. The dynamical transitions are studied both as a function of the repulsive coupling and the natural frequency of the oscillator. We deduce the IPS, OPS, and NAD states along with their stability condition. We also deduce the stability conditions for the SNIPER and pitchfork bifurcations, which are found to agree well with the simulation boundaries, using linear stability analysis. Coupled nonidentical Stuart-Landau oscillators result in a rich bifurcation diagram with quasiperiodic oscillation, periodic oscillation, and steady state as a function of the repulsive coupling strength. In addition to the SNIPER and the homoclinic bifurcations, a torus bifurcation mediates the transition from the quasiperiodic oscillation to the periodic oscillation. Multistability between two different quasiperiodic oscillations, periodic oscillations, and that between OD and periodic oscillation is also observed. The dynamical transitions are studied both as a function of the repulsive coupling and the frequency disparity using a uniform distribution of natural frequencies by varying the range of distribution. We also extended our results to N-coupled identical and nonidentical Stuart-Landau oscillators and two coupled FitzHugh-Nagumo models in the Sec. VI and VII, respectively to corroborate the generic nature of the effect of the limiting factor in the employed coupling configuration.

The plan of the paper is as follows. In Sec. II we present the model under consideration. In Sec. III we discuss the emergent collective dynamical states obtained from numerical integration of the coupled identical Stuart-Landau oscillators (1). In Sec. IV we deduce the observed dynamical states and the governing evolution equation for the perturbations that determines the stability of the observed dynamical states. In Sec. V we discuss the collective dynamical states exhibited by the coupled nonidentical Stuart-Landau oscillators with frequency mismatch. Finally, we summarize our results in Sec. VI.

II. MODEL

We consider the paradigmatic model of Stuart-Landau limit-cycle oscillators. Many nonlinear dynamical systems near the Hopf bifurcation can be approximated as the Stuart-Landau oscillator. Diffusive coupling among the x variables is coupled repulsively to the evolution equation of the dissimilar (conjugate) variables of the Stuart-Landau oscillators as

$$\dot{z}_j = (1 + i\omega_j - |z_j|^2)z_j - i\varepsilon Re(z_k - az_j), \tag{1}$$

where $z_j = x_j + iy_j$ for $j, k = 1, 2$ $(j \neq k)$. x_j and y_j are the state variables of the jth system. ω_j is the natural frequency of the jth oscillator. $\varepsilon > 0$ is the strength of the repulsive coupling. Note that the coupling is only in the y_j variable via the x_k variable. The limiting factor a ranging from $0 < a \leqslant 1$ limits the interaction and diffusion of the x_j and x_k variables. Note that the limiting factor also determines the nature of the coupling. $a = 1$ corresponds to a normal diffusive coupling, whereas $a = 0$ refers to a direct coupling scheme, bridging the direct coupling and the normal diffusive interaction.

III. NUMERICAL RESULTS

The coupled Stuart-Landau oscillators (1) are numerically solved using the Runge-Kutta fourth-order integration scheme with a time step of 0.01 to obtain the time series and phase portraits of the observed dynamical states, including the two-parameter phase diagrams. One-parameter bifurcation diagrams are obtained using the XPPAUT software. To begin with, we have depicted the time series (left column) and the corresponding phase portraits (right column) of the coupled identical Stuart-Landau oscillators for $\omega_j = \omega = 0.5$ and the limiting factor $a = 0.5$ in Fig. 1 for different values of the repulsive coupling strength ε. In-phase oscillations exhibited by the Stuart-Landau oscillators for $\varepsilon = 0.5$ are depicted in Figs. 1(a) and 1(b), while the out-of-phase oscillations exhibited by the Stuart-Landau oscillators for $\varepsilon = 1.0$ are depicted

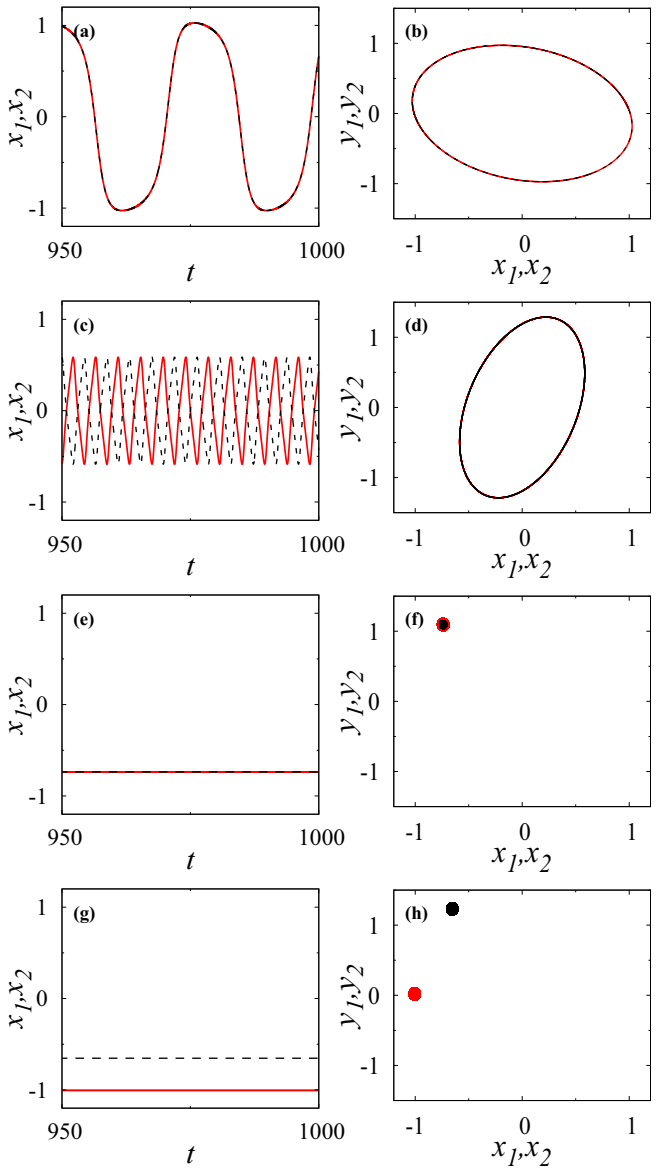

FIG. 1. Time series (left column) and the corresponding phase portraits (right column) of the coupled identical Stuart-Landau oscillators for $\omega_j = \omega = 0.5$ and the limiting factor $a = 0.5$: (a, b) in-phase oscillations for $\varepsilon = 0.5$, (c, d) out-of-phase oscillations for $\varepsilon = 0.5$, (e, f) nontrivial amplitude death for $\varepsilon = 1.15$, and (g, h) oscillation death for $\varepsilon = 3.0$.

in Figs. 1(c) and 1(d). Note that both the in-phase and out-of-phase oscillations coexist, resulting in the bistability between them, in a large range of the coupling strength. Nontrivial amplitude death is depicted in Figs. 1(e) and 1(f) for $\varepsilon = 1.15$, which coexists with the out-of-phase oscillations in a certain range of ε, after which the former survives as the only stable state for further larger ε. The oscillation death state is depicted in Figs. 1(g) and 1(h) for $\varepsilon = 3.0$.

We have depicted the one-parameter bifurcation diagrams to understand the nature of the bifurcation transitions among the observed dynamical states for different values of the limiting factor a as a function of the repulsive coupling strength ε in Fig. 2. The bifurcation diagram for the limiting factor $a = 1$, depicted in Fig. 2(a), elucidates the coexisting in-phase (lines connected by filled circles) and out-of-phase (lines connected by filled squares) oscillations in the entire explored range of coupling strength. However, rich bifurcations are observed upon decreasing the value of the limiting factor. There is a transition from the in-phase oscillatory state to the nontrivial amplitude death (indicated by solid red line) via a SNIPER bifurcation at $\varepsilon = 0.816$, which coexists with the out-of-phase oscillatory state in the explored range of ε [see Fig. 2(b)] depicted for $a = 0.4$. Unstable steady states are indicated by dotted lines. Further, the NAD state is destabilized at $\varepsilon = 1.18$, resulting in the OD state via a pitchfork (PF) bifurcation, which remains stable in the range of $\varepsilon \in (1.18, 4)$. Furthermore, the OPS state loses its stability via a homoclinic (Hc) bifurcation at $\varepsilon = 1.9$. Unstable oscillatory states are indicated by open triangles.

Further decrease in the value of the limiting factor facilitates the emergence of the NAD state in a rather larger range of the coupling strength as shown in Fig. 2(c) for $a = 0.28$. In particular, the nontrivial amplitude death state coexists with the out-of-phase oscillatory state in the range $\varepsilon \in (0.71, 1.65]$, while the former emerges as the only stable state for $\varepsilon \in (1.65, 3.2)$, as the latter loses its stability via the homoclinic bifurcation at $\varepsilon = 1.65$. It is to be noted that the OD state for $a = 0.28$ onsets via a saddle-node (SN) bifurcation. Thus, it is clearly evident that the limiting factor in the intrinsic variable that destabilizes the stable steady states facilitating the revival of oscillations in the normal diffusive coupling can also indeed surprisingly lead to the counterintuitive effect of stabilizing the nontrivial steady state via the SNIPER bifurcation, while the diffusion among the x variables is repulsively coupled to the evolution equation of the dissimilar (conjugate) variables.

One-parameter bifurcation diagrams as a function of ω for two different values of the limiting factor a are depicted in Fig. 3. The dynamical states and the bifurcation transitions are similar to those observed in Figs. 2(b) and 2(c), except that the bifurcation transitions are reversed in Figs. 3(a) and 3(b) as the value of ω is increased in the range $\omega \in (0, 3)$. It is to be noted that the stable NAD state is observed only in a narrow range of $\varepsilon \in (0.93, 1.21)$ in Fig. 3(a) for $a = 0.7$, whereas the spread of the NAD state is increased to the range $\varepsilon \in (0.98, 2)$ in Fig. 3(b) for $a = 0.4$. Hence, it is clear that the limiting factor favors the onset of the NAD state and its spread in a large range of the parameter space, in contrast to its effect of reviving oscillations in normal diffusive coupling.

Two-parameter phase diagrams in the (ε, a) space are depicted in Fig. 4 to unravel the global dynamical transitions. The pink (gray) shaded region, indicated as M1, corresponds to the bistable region between the in-phase and out-of-phase oscillatory states. The parameter space below the solid line corresponds to the NAD state. The solid line is the SNIPER bifurcation line across which the in-phase oscillation loses its stability, resulting in the manifestation of the NAD state. The dotted-dashed line corresponds to the homoclinic bifurcation curve at which the out-of-phase oscillation loses its stability, resulting in the monostable region of the NAD state for small values of a in Fig. 4(a) for $\omega = 0.5$ and in the entire explored range of the parameters in Fig. 4(b) for $\omega = 1$. The parameter space between the solid and dotted-dashed lines, indicated as

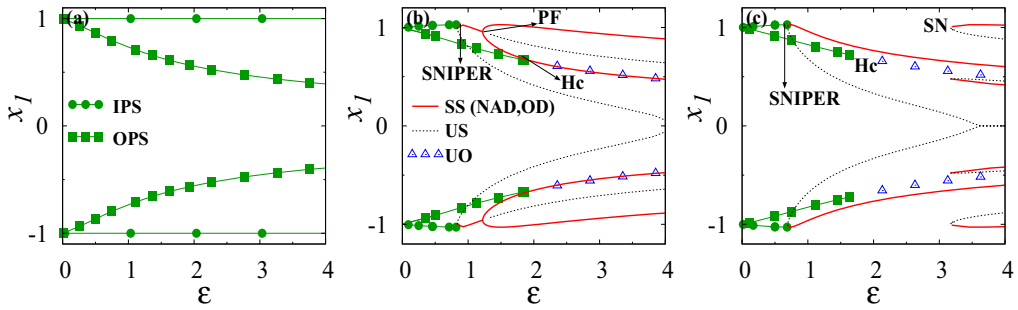

FIG. 2. One-parameter bifurcation diagrams of the coupled identical Stuart-Landau oscillators (1) as a function of the repulsive coupling ε for different values of the limiting factor a. (a) $a = 1$, (b) $a = 0.4$, and (c) $a = 0.28$ for $\omega = 0.5$. Stable in-phase (out-of-phase) oscillatory states are represented by lines connected by filled circles (squares), while stable steady states (SS) are represented by solid red line. Unstable oscillatory states (UO) are indicated by open triangles, while the unstable steady states (US) are represented by dotted lines. The in-phase oscillatory state loses its stability via the SNIPER bifurcation, while the out-of-phase oscillatory state loses its stability via the homoclinic (Hc) bifurcation.

M2, correspond to the bistable region between the out-of-phase oscillatory state and the NAD state. The coupling is the normal repulsive and diffusive coupling for $a = 1$, which results only in the bistable region M1, as observed in the one-parameter bifurcation diagram [see Fig. 2(a)].

Nevertheless, as the value of the limiting factor a is decreased, there is a transition from the M1 to M3 region via the M2 region for the intermediate values of a [see Fig. 4(a)] and then to the monostable OD state as a function of ε. The parameter space indicated by M3 is the bistable region between the OPS and OD states. The region enclosed by the pitchfork bifurcation curve, represented by the dotted line, and saddle-node bifurcation curve, the line connected by open squares, corresponds to the OD state. The bistability between the OD and NAD states, indicated by M4, is observed in a narrow range of a for large values of ε. However, for a large $\omega = 1$, there is a transition from the M1 to M2 region and then to the monostable NAD region, as observed in the entire phase diagram in Fig. 4(b) in the range of the limiting factor $a \in (0, 1)$. It is also evident from the phase diagram (see Fig. 4) that decreasing the value of the limiting factor favors the NAD state in a rather larger region of the parameter space, corroborating the results observed in the one-parameter bifurcation diagrams (see Fig. 2). Thus, the effect of the limiting factor in the intrinsic variable in our study is in complete contrast to that of normal diffusive coupling [17]. The limiting factor facilitates the manifestation of the stable NAD state from the stable oscillatory state in the employed coupling configuration, whereas in the normal diffusive coupling it facilitates the manifestation of the stable oscillatory state from distinct stable steady states [13,18,20–22].

Two-parameter phase diagrams in the (ε, ω) parameter space are depicted in Figs. 5(a) and 5(b) for $a = 0.7$ and 0.5, respectively, to understand the influence of the natural frequency ω. The dynamical states and the multistable regions along with the bifurcation curves are similar to those observed in Fig. 4. For large values of ω, there is a transition from M1 to M2 and then to the NAD state, as observed in Fig. 4(b). However, small values of ω favor the onset of the OD state, thereby resulting the multistable state M3 and monostable state OD. Consequently, there is a transition from M1 to M3 and then to the OD state as a function of ε in Figs. 5(a) and

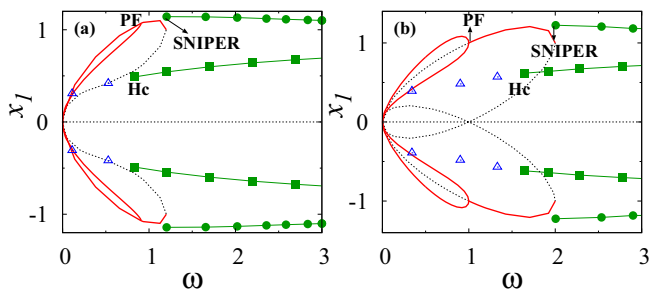

FIG. 3. One-parameter bifurcation diagrams of the coupled identical Stuart-Landau oscillators (1) as a function of the ω for different values of the limiting factor a: (a) $a = 0.7$ and (b) $a = 0.4$. The repulsive coupling $\varepsilon = 4$. The dynamical states and their bifurcation transitions are similar to those in Fig. 2.

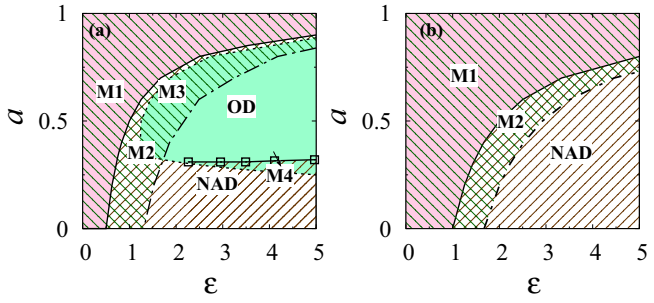

FIG. 4. Two-parameter phase diagrams in the (ε, a) parameter space of the coupled identical Stuart-Landau oscillators for different ω: (a) $\omega = 0.5$ and (b) $\omega = 1$. The parameter regions marked as M1 and M2 correspond to the bistable regions between the in-phase and out-of-phase oscillatory states, and the out-of-phase oscillatory state and the nontrivial amplitude death state, respectively. Coexistence of oscillation death and out-of-phase oscillatory state are denoted as $M3$, whereas the coexistence of oscillation death and nontrivial amplitude death state are marked as $M4$. The dotted line and line connected by open squares correspond to the pitchfork and saddle-node bifurcations, respectively. The solid black line corresponds to the SNIPER bifurcation curve, while the dotted-dashed black line corresponds to the homoclinic bifurcation curve.

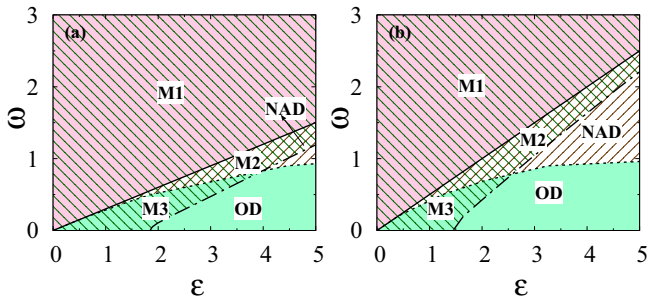

FIG. 5. Two-parameter phase diagrams in the (ε, ω) parameter space of the coupled identical Stuart-Landau oscillators for different values of the limiting factor: (a) $a = 0.7$ and (b) $a = 0.5$. The dynamical states and the multistable regions along with the bifurcation curves are similar to those in Fig. 4.

$$x_1^\star = \frac{\cos[\sqrt{\omega(K+\omega)}(t+C_2)]}{\sqrt{C_1 e^{-2t\lambda} + \frac{\lambda^2[K - K\cos(2\sqrt{\omega(K+\omega)}(t+C_2)) + 2\omega] + \omega(2\omega^2+K^2+3K) - K\lambda\sin(2\sqrt{\omega(K+\omega)}(t+C_2))}{2\omega\lambda(\lambda^2+\omega(K+\omega))}}}, \tag{2a}$$

$$y_1^\star = \frac{\sqrt{K+\omega}\sin(\sqrt{\omega(K+\omega)}(t+C_2))}{\sqrt{\omega\left[C_1 e^{-2t\lambda} + \left(\frac{\lambda^2[K - K\cos(2\sqrt{\omega(K+\omega)}(t+C_2)) + 2\omega] + \omega(2\omega^2+K^2+3K) - K\lambda\sin(2\sqrt{\omega(K+\omega)}(t+C_2))}{2\omega\lambda(\lambda^2+\omega(K+\omega))}\right)\right]}}, \tag{2b}$$

where $K = \varepsilon(a-1)$ for the symmetric subspace, $K = \varepsilon(1+a)$ for the antisymmetric subspace, and C_1 and C_2 are the integration constants. Note that $(x_1^\star, y_1^\star)$ in Eq. (2) exhibit periodic oscillation when $K + \omega > 0$. For $\omega < \varepsilon(1-a)$, the solutions in Eq. (2) manifest as a nontrivial steady state. In the asymptotic limit $t \to \infty$, $x_{1,2}^\star$ and $y_{1,2}^\star$ tend to a constant value, leading to the nontrivial steady state given by

$$x_1^\star = x_2^\star = \sqrt{\frac{(\epsilon\omega(1-a))}{M_1} + M_2},$$
$$y_1^\star = y_2^\star = \frac{1}{\omega^2}\left(\omega x_1^\star + x_1^{\star 3}\epsilon(a-1)\right), \tag{3}$$

where

$$M_1 = \epsilon^2(1-a)^2,$$
$$M_2 = \frac{\sqrt{[(2\omega)^2 - 4(\omega^4 + (a-1)\omega^3)]M_1 + \omega^2}}{2M_1}. \tag{4}$$

Now to analyze the stability of the symmetric (in-phase oscillatory state and the nontrivial amplitude death state) and the antisymmetric (out-of-phase oscillation) states, we perturb the periodic solutions corresponding to the symmetric state as

$$x_1 = x_1^\star + \eta_1, \quad y_1 = y_1^\star + \eta_2, \tag{5a}$$
$$x_2 = x_1^\star + \zeta_1, \quad y_2 = y_1^\star + \zeta_2, \tag{5b}$$

5(b). It is again evident that decreasing the limiting factor results in a more pronounced region of the NAD state, even in the (ε, ω) parameter space [see Fig. 5(b)], corroborating its counterintuitive effect in the employed coupling configuration. We now analytically deduce the stability curves, namely, the homoclinic and the SNIPER bifurcation curves, in the following.

IV. COLLECTIVE DYNAMICAL STATES AND THEIR STABILITY

The state variables in the in-phase synchronization manifold, where $x_1 = x_2$ and $y_1 = y_2$, and those in the out-of-phase synchronization manifold, characterized by $x_1 = -x_2$ and $y_1 = -y_2$, can be deduced as

and those for the antisymmetric state as

$$x_1 = x_1^\star + \eta_1, \quad y_1 = y_1^\star + \eta_2, \tag{6a}$$
$$x_2 = -x_1^\star + \zeta_1, \quad y_2 = -y_1^\star + \zeta_2, \tag{6b}$$

where $\eta_i, \zeta_i, i = 1, 2$ are the perturbations. By substituting the above perturbations in the system equation (1) and by linearizing, one can deduce the governing equation of motion for the perturbations as

$$\dot{\eta}_1 = \left(\lambda - 3x_1^{\star 2} - y_1^\star\right)\eta_1 - (\omega + 2x_1^\star y_1^\star)\eta_2, \tag{7a}$$
$$\dot{\eta}_2 = \left(\lambda - x_1^{\star 2} - 3y_1^\star\right)\eta_2 + (\omega - 2x_1^\star y_1^\star)\eta_1 - \epsilon(\zeta_1 - a\eta_1), \tag{7b}$$
$$\dot{\zeta}_1 = \left(\lambda - 3x_1^{\star 2} - y_1^\star\right)\zeta_1 - (\omega + 2x_1^\star y_1^\star)\zeta_2, \tag{7c}$$
$$\dot{\zeta}_2 = \left(\lambda - x_1^{\star 2} - 3y_1^\star\right)\zeta_2 + (\omega - 2x_1^\star y_1^\star)\zeta_1 - \epsilon(\eta_1 - a\zeta_1). \tag{7d}$$

One can determine the stability of the observed collective dynamical states by solving the above system of evolution equations for the perturbations corresponding to the dynamical states as a function of the repulsive coupling strength and the limiting factor. In particular, one can determine the stable region of the nontrivial amplitude death state in the parameter space by substituting the steady state (x_1^*, y_1^*) (3) in the evolution equations for the perturbations and trace the regions where the perturbations die out, which will lead to the SNIPER bifurcation curve.

Nevertheless, the SNIPER and the pitchfork bifurcation curves, in between which the NAD is stable, can be obtained by deducing the stability condition for the NAD state through the linear stability analysis. The Jacobian matrix of the

perturbed system of equations, Eqs. (7), corresponding to the NAD state can be obtained as

$$J = \begin{bmatrix} 1-3x_1^{\star 2}-y_1^{\star 2} & -\omega-2x_1^{\star}y_1^{\star} & 0 & 0 \\ \omega-2x_1^{\star}y_1^{\star}+\epsilon a & 1-x_1^{\star 2}-3y_1^{\star 2} & -\epsilon & 0 \\ 0 & 0 & 1-3x_1^{\star 2}-y_1^{\star 2} & -\omega-2x_1^{\star}y_1^{\star} \\ -\epsilon & 0 & \omega-2x_1^{\star}y_1^{\star}+\epsilon a & 1-x_1^{\star 2}-3y_1^{\star 2} \end{bmatrix}. \tag{8}$$

The corresponding eigenvalues for the above Jacobian matrix can be expressed as

$$\lambda_{1,2} = 1-2x_1^{\star 2}-2y_1^{\star 2} \pm \sqrt{\left(x_1^{\star 2}+y_1^{\star 2}\right)^2-\omega^2-\epsilon(1+a)(\omega+2x_1^{\star}y_1^{\star})}, \tag{9a}$$

$$\lambda_{3,4} = 1-2x_1^{\star 2}-2y_1^{\star 2} \pm \sqrt{\left(x_1^{\star 2}+y_1^{\star 2}\right)^2-\omega^2+\epsilon[\omega(1-a)-2(1+a)x_1^{\star}y_1^{\star}]}. \tag{9b}$$

By substituting the NAD state [Eq. (3)] in the above eigenvalue equations, one can deduce the stability condition for the SNIPER bifurcation curve as

$$a = \frac{\epsilon-\omega}{\epsilon} \tag{10}$$

and the pitchfork bifurcation curve as

$$\begin{aligned} &2a^4\epsilon^3\omega^2+a^3\epsilon^2\omega(4\omega^2-7\epsilon\omega-2)+a^2\epsilon[2\omega^4-9\epsilon\omega^3 \\ &-(2+9\epsilon^2)\omega^2+4\epsilon\omega+4Q_1]-a[2\epsilon\omega^4 \\ &-6\epsilon^2\omega^3+(5\epsilon^2-2)\epsilon\omega^2 \\ &+2(\epsilon^2-2Q_1)\omega+5\epsilon Q_1]+\epsilon(\epsilon^2\omega^2-\epsilon\omega^3+Q_1)=0, \end{aligned} \tag{11}$$

where $Q_1 = \sqrt{(a-1)^2\epsilon^2\omega^3((a-1)\epsilon+\omega)}$. These critical curves corresponding to the SNIPER and the pitchfork bifurcation curves that enclose the stable NAD state and these bifurcation curves are found to agree with the simulation results in Figs. 4 and 5.

The stable region of in-phase and out-of-phase oscillations can also be determined by investigating the asymptotic states of the evolution equations for the perturbations corresponding to the in-phase and out-of-phase oscillatory states, which will also result in the SNIPER and homoclinic bifurcation curves, respectively. One can also use the Floquet theorem to determine the stability of the limit-cycle oscillations (in-phase and out-of-phase oscillations). Integrating the above system of equations, one can determine the Floquet multipliers from the fundamental matrix [25]. The Floquet multipliers for in-phase (out-of-phase) oscillation as a function of the repulsive coupling strength ε for different values of the limiting factor can also result in the SNIPER (homoclinic) bifurcation curve in the (ε, a) parameter space. Note that in the symmetric manifold in-phase oscillation loses its stability and manifests as the nontrivial amplitude death state via the SNIPER bifurcation curve, while in the antisymmetric manifold the out-of-phase oscillation loses its stability via the homoclinic bifurcation.

The SNIPER and the homoclinic bifurcation curves in Fig. 4 are also verified from the XPPAUT software, which are found to agree very well with the stability curves obtained from the evolution equation for the perturbations corresponding to the distinct dynamical states.

V. COUPLED NONIDENTICAL OSCILLATOR DYNAMICS

In this section we introduce the parameter mismatch in terms of nonidentical frequencies among the two coupled Stuart-Landau oscillators in (1) and investigate the effect of heterogeneity on the collective dynamics exhibited by the coupled identical Stuart-Landau oscillators. We have depicted the one-parameter bifurcation diagrams of the coupled nonidentical Stuart-Landau oscillators as a function of the repulsive coupling for the frequency mismatch $\Delta\omega = 0.3$ ($\omega_1 = 1$ and $\omega_2 = 1.3$) in Figs. 6(a) and 6(b) for the values of the limiting factor $a = 1$ and $a = 0.6$, respectively. As in Fig. 2, stable (unstable) oscillatory states are depicted as filled (unfilled) symbols, while stable (unstable) steady states are represented by solid (dotted) lines. Two different torus bifurcations Tr1 and Tr2 mediate the transition from two different quasiperiodic oscillations QP1 and QP2 to two different oscillatory states Os1 and Os2, respectively (see Fig. 6). We observe no other dynamical states and transitions in the explored range of the bifurcation diagram for the limiting factor $a = 1$ [see Fig. 6(a)]. However, upon decreasing the value of the limiting factor to $a = 0.6$, there is a transition from Os1 to the oscillation death (OD) state via the SNIPER bifurcation as a function of ε in addition to the observed dynamical transition from QP1 to Os1 [see Fig. 6(b)]. Further, Os2 loses its stability via the homoclinic bifurcation as in the case of coupled identical

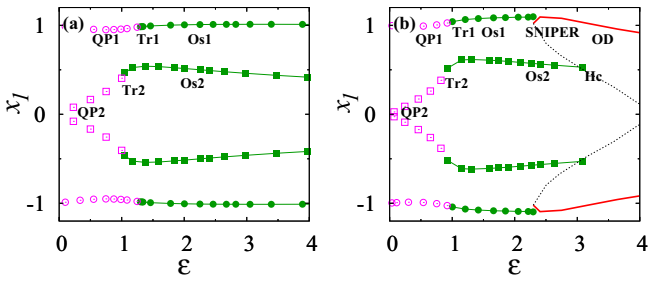

FIG. 6. One-parameter bifurcation diagrams as a function of the repulsive coupling strength ε of the coupled Stuart-Landau oscillators with the frequency mismatch $\Delta\omega = 0.3$. The limiting factor (a) a = 1 and (b) a = 0.6. The bifurcation diagrams are obtained using the software XPPAUT. The lines connected with filled circles and squares indicate the stable oscillatory states Os1 and Os2, respectively. The empty circles and squares represent the quasiperiodic states QP1 and QP2, respectively. The solid red and dashed black lines, respectively, indicate the stable and unstable steady states.

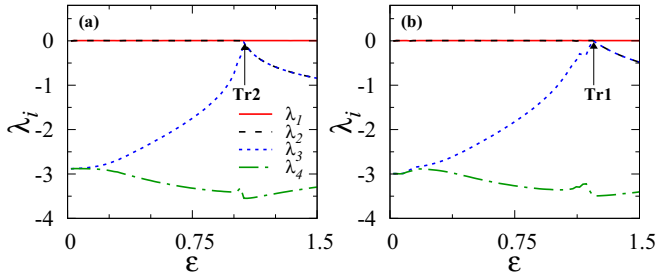

FIG. 7. Lyapunov spectrum in the range of $\varepsilon \in (0, 1.5)$ corroborating the quasiperiodic attractors in Fig. 6(a).

Stuart-Landau oscillators. Thus it is evident that limiting the intrinsic variable in the coupling facilitates the manifestation of steady states, here oscillation death, in contrast to its effect observed in Ref. [18]. It is also to be noted that the parameter mismatch favors the onset of the heterogeneous steady states rather than the nontrivial steady state.

The quasiperiodic nature of the two different quasiperiodic oscillations QP1 and QP2 is indeed confirmed by the torus bifurcations at Tr2 and Tr1 [see Fig. 6(a)]. Nevertheless, we have also corroborated it using the Lyapunov spectrum depicted in Fig. 7, where the four Lyapunov exponents of the two coupled nonidentical Stuart-Landau oscillators are plotted as a function of the repulsive coupling $\varepsilon \in (0, 1.5)$ for $a = 1$. The values of the other parameters are the same as in Fig. 6(a). $\lambda_1 = \lambda_2 \approx 0$ corroborates the quasiperiodic nature of QP1 and QP2. The Lyapunov spectrum shown in Figs. 7(a) and 7(b) are obtained for two distinct initial conditions that are chosen on the two distinct quasiperiodic attractors, which lose their stability via the torus bifurcations Tr2 and Tr1 at $\varepsilon = 1.05$ and 1.3, respectively.

The representative time series (left column) and phase portraits (right column) of the different coexisting dynamical states observed in the bifurcation diagrams are depicted in Figs. 8–11 for different ε. The values of the other parameters are the same as in Fig. 6(b). Solid and dashed lines correspond to the dynamics of the first and second oscillators, respectively. Time series and phase portraits of two different coexisting quasiperiodic attractors are shown in Fig. 8 for $\varepsilon = 0.5$. The coexisting limit cycles and the quasiperiodic oscillations for $\varepsilon = 0.95$ are depicted in Fig. 9. Similarly, coexisting two different limit-cycle oscillations are plotted in Fig. 10 for $\varepsilon = 1.2$. The coexisting limit-cycle oscillation and heterogeneous steady states are depicted in Fig. 11 for $\varepsilon = 2.5$.

Two-parameter phase diagrams in the (ε, a) space are depicted in Figs. 12(a) and 12(b) for $\Delta\omega = 0.1$ ($\omega_1 = 1$ and $\omega_2 = 1.1$) and 0.3, respectively, to unravel the global bifurcation transitions. The unshaded region, indicated as R1, corresponds to the region of coexisting quasiperiodic attractors QP1 and QP2. The gray shaded region between the dashed lines indicated as R2 is the bistable region between the QP1 and Os2 states. The region marked R3 lying between the dashed and solid lines is the bistable region between the Os1 and Os2 states. The region between the solid and dotted-dashed lines, indicated as R4, corresponds to the bistable region between the OD and Os2 states, while the region below

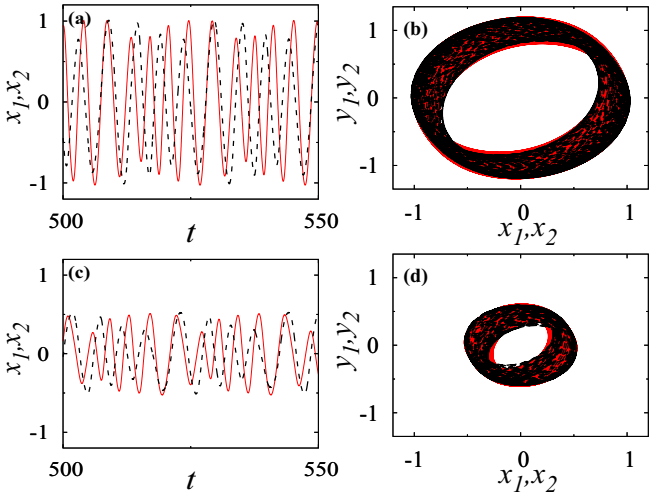

FIG. 8. Time series (left column) and phase portraits (right column) of the coupled Stuart-Landau oscillators with the frequency mismatch $\Delta\omega = 0.3$. The limiting factor $a = 0.6$ and the repulsive coupling strength $\varepsilon = 0.5$.

the dotted-dashed line corresponds to the monostable heterogeneous steady state (OD). Note that dashed lines correspond to the torus bifurcation curves Tr1 and Tr2 in the order of their emergence, while the solid line is the SNIPER bifurcation line across which Os1 loses its stability, resulting in the manifestation of the oscillation death state. The dotted-dashed line corresponds to the homoclinic bifurcation line at which the Os2 loses its stability, leading to the monostable region of oscillation death state. All these bifurcation curves are obtained using the XPPAUT software, which has also been verified numerically. There is a transition from R1 to R3 via R2 as a function of ε for larger values of the limiting factor a. As the value of the limiting factor is decreased, one can observe the transition to the oscillation death states, resulting

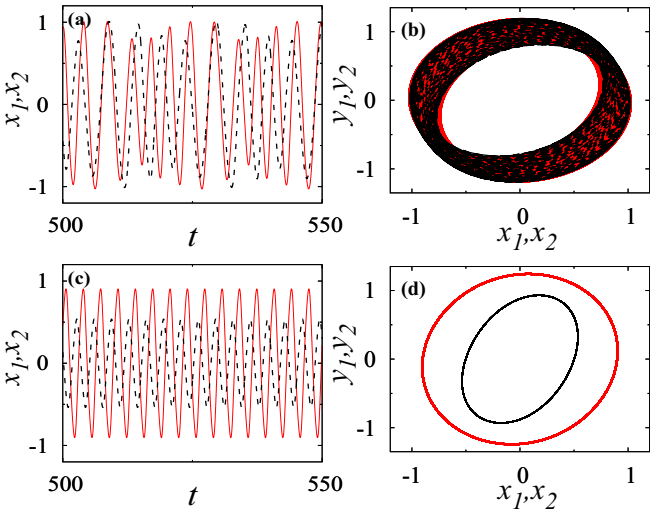

FIG. 9. Time series (left column) and phase portraits (right column) of the coupled Stuart-Landau oscillators with the frequency mismatch $\Delta\omega = 0.3$. The limiting factor $a = 0.6$ and the repulsive coupling strength $\varepsilon = 0.95$.

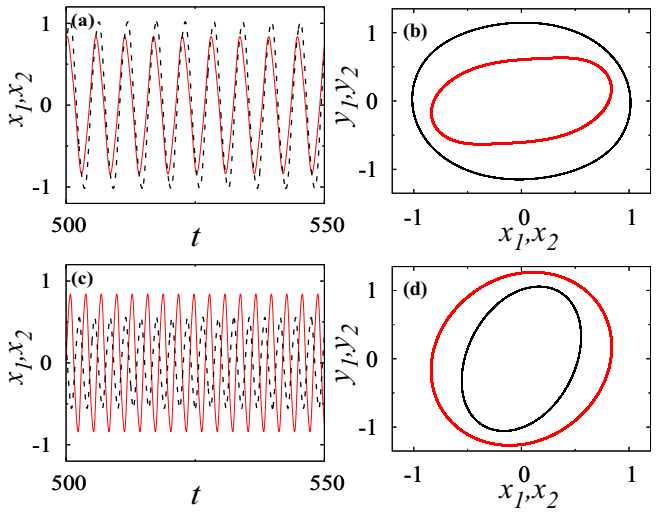

FIG. 10. Time series (left column) and phase portraits (right column) of the coupled Stuart-Landau oscillators with frequency mismatch $\Delta\omega = 0.3$. The limiting factor $a = 0.6$ and the repulsive coupling strength $\varepsilon = 1.2$.

in the bistable region R4 in addition to the above dynamical transitions. Increase in the frequency mismatch facilitates the quasiperiodic attractors QP1 and QP2 in a larger parameter space while reducing the bistable region R3.

Two-parameter phase diagrams in the $(\varepsilon, \Delta\omega)$ space are depicted in Figs. 13(a) and 13(b) for $a = 0.7$ and 0.5, respectively, to elucidate the role of frequency disparity on the observed dynamical states. The bifurcation transitions and the bistable regions are similar to those observed in Fig. 12. In the entire explored range of $\Delta\omega$, there is a transition from R1 to the OD state via R2, R3, and R4 in both Figs. 13(a) and 13(b). However, it is evident that spread of the OD state increased to a large extent even for a small decrease

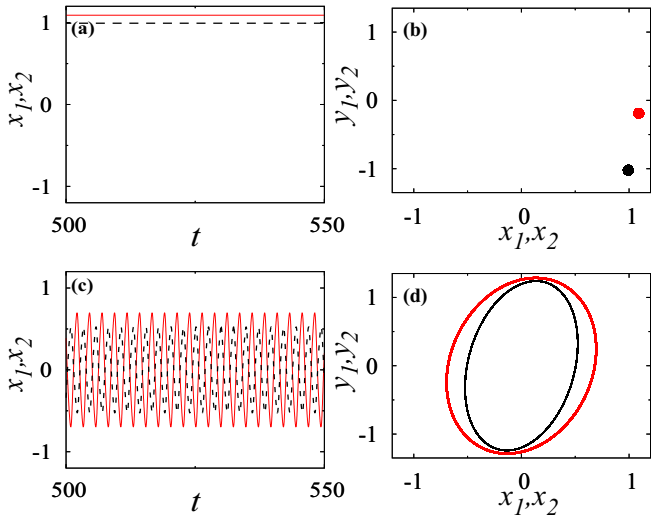

FIG. 11. Time series (left column) and phase portraits (right column) of the coupled Stuart-Landau oscillators with the frequency mismatch $\Delta\omega = 0.3$. The limiting factor $a = 0.6$ and the repulsive coupling strength $\varepsilon = 2.5$.

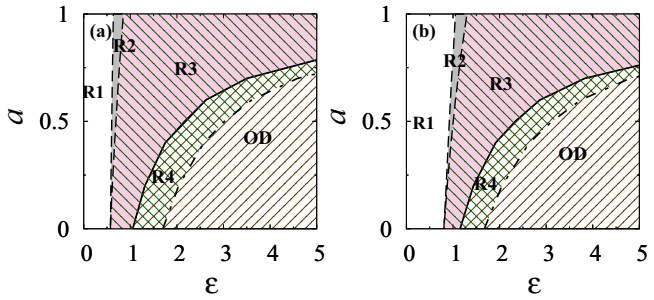

FIG. 12. Two-parameter phase diagram in the (ε, a) parameter space of the coupled Stuart-Landau oscillators with frequency mismatch $\Delta\omega = 0.1$ and 0.3. Unshaded region, indicated as R1, corresponds to the region of coexisting quasiperiodic attractors QP1 and QP2. The gray shaded region between the dashed lines (torus bifurcation curve) indicated as R2 is the bistable region between QP1 and Os2 states. The region marked as R3 lying between the dashed and solid (SNIPER bifurcation curve) lines is the bistable region between the Os1 and Os2 states. The region, indicated as R4, between the solid and dotted-dashed (homoclinic bifurcation curve) lines correspond to the bistable region between OD and Os2 states, while the region below the dotted-dashed line corresponds to the monostable heterogeneous steady state (OD). The bifurcation curves are obtained using the XPPAUT software. Shaded regions correspond to the numerical results.

in the limiting factor a [see Fig. 13(b)]. Further, it is also evident that the frequency disparity favors the onset of the OD state rather than the NAD state, as already pointed out.

VI. COUPLED FITZHUGH-NAGUMO OSCILLATORS

In order to elucidate the robustness of the effect of the limiting factor in the employed coupling, where the x variables are coupled repulsively to the dissimilar variables, we consider the two coupled paradigmatic model of the FitzHugh-Nagumo oscillator, whose evolution equation is represented as

$$\begin{aligned} \beta\dot{x}_i &= x_i - {x_i}^3/3 - y_i, \\ \dot{y}_i &= x_i + \alpha - \epsilon(x_j - a x_i), \end{aligned} \tag{12}$$

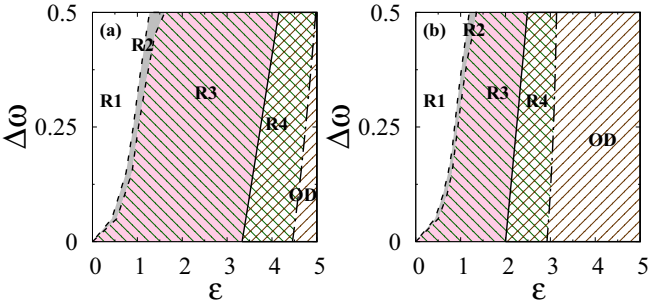

FIG. 13. Two-parameter phase diagrams in the $(\varepsilon, \Delta\omega)$ parameter space of the coupled Stuart-Landau oscillators for (a) $a = 0.7$ and (b) 0.5. The dynamical states and the bifurcation curves are similar to those observed in Fig. 12.

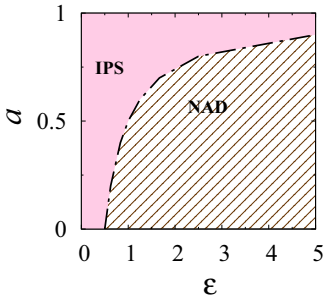

FIG. 14. Two-parameter phase diagram in (ϵ, a) parameter space of the coupled FitzHugh-Nagumo model, Eq. (12), for $\alpha = 0.5$ and $\beta = 0.05$. The pink (gray) shaded region is the IPS state, while the region below the dotted-dashed line, SNIPER bifurcation curve, is the NAD state.

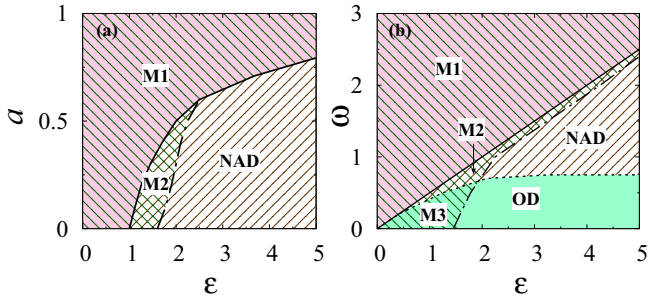

FIG. 15. Two-parameter phase diagrams of $N = 100$ globally coupled identical Stuart-Landau oscillators, Eq. (13) in (a) (ϵ, a) parameter space for $\omega = 1$, and (b) (ϵ, ω) parameter space for $a = 0.5$. The dynamical states and their bifurcation transitions are similar to those observed in Fig. 4.

where $i, j = 1, 2 (i \neq j)$. x_i and y_i are the activator and inhibitor variables, α is a threshold parameter, and β characterizes the timescale of separation. a is the limiting factor. The FitzHugh-Nagumo model is a mathematical description of the qualitative features of the nervous impulse conduction in the neural cell [26]. We have fixed $\alpha = 0.5$ and $\beta = 0.05$. The two-parameter phase diagram of the two coupled FitzHugh-Nagumo oscillator in the (ε, a) parameter space is depicted in Fig. 14. For $a = 1$, only IPS is observed in the entire explored range of the repulsive coupling strength $\varepsilon \in (0, 5)$. Nevertheless, it is evident that decreasing a leads to the onset of the NAD state and also favors the spread of the NAD state to a large range of the parameter space (see Fig. 14), thereby corroborating the counterintuitive effect of stabilizing the nontrivial steady state via the SNIPER bifurcation, indicated by dotted-dashed line, generalizing the results observed in the main part of the manuscript.

VII. ENSEMBLE OF GLOBALLY COUPLED STUART-LANDAU OSCILLATORS

We consider N globally coupled Stuart-Landau oscillators to further illustrate the generic nature of the effect of the limiting factor facilitating the onset of the NAD state in coupled identical oscillators and the OD state in coupled oscillators with heterogeneity. The evolution equation for the N globally coupled Stuart-Landau oscillators is represented as

$$\dot{z}_j = (1 + i\omega_j - |z_j|^2) z_j - i\frac{\varepsilon}{N}\sum_{k=0}^{N} Re(z_k - a z_j), \qquad (13)$$

where $z_j = x_j + iy_j$ and $j, k = 1, 2, \ldots, N$. The parameters are the same as in the two coupled Stuart-Landau oscillators presented in the main part of the manuscript. Two-parameter phase diagrams are depicted in (ε, a) space for $\omega = 1$ in Fig. 15(a) and in (ε, ω) space for $a = 0.5$ in Fig. 15(b) to corroborate the generic nature of the effect of the limiting factor as a function of the repulsive coupling strength ε in an ensemble of coupled nonlinear oscillators. The observed dynamical states and their bifurcation transitions for $N = 100$ globally coupled Stuart-Landau oscillators strongly resemble those observed in Fig. 4 for two coupled Stuart-Landau oscillators in both (ε, a) and (ε, ω) parameter spaces, corroborating the counterintuitive effect of the limiting factor in inducing the NAD and symmetry-breaking OD states, when the x variables are coupled repulsively to the dissimilar variables, which is known to facilitate the revival of oscillation from the quenched states in the case of normal diffusive coupling.

Two-parameter phase diagrams are depicted in the (ε, a) space for $\Delta\omega = 0.3$ in Fig. 16(a) and in the $(\varepsilon, \Delta\omega)$ space for $a = 0.5$ in Fig. 16(b) to illustrate the interplay of the frequency heterogeneity and the limiting factor. We have distributed the frequency between ω and $\omega + \Delta\omega$ uniformly to all the oscillators. Here, we have fixed $\omega = 1$. The transition from two distinct quasiperiodic oscillations, indicated as R1, to the OD state is observed in both phase diagrams. For $a = 1$, only the quasiperiodic orbits are observed in the entire explored range of the repulsive coupling strength $\varepsilon \in (0, 5)$. Nevertheless, decreasing the limiting factor is found to facilitate the onset of the symmetric OD state and the spread of the latter to a large region of the parameter space [see Fig. 16(a)] even in $N = 100$ globally coupled Stuart-Landau oscillators with frequency disparity. Further, there is a transition from R1 to the OD state in the entire phase diagram in the $(\varepsilon, \Delta\omega)$ parameter space in Fig. 16(b). Again, the effect of the limiting factor a and the frequency mismatch in an ensemble of globally coupled Stuart-Landau oscillators is similar to

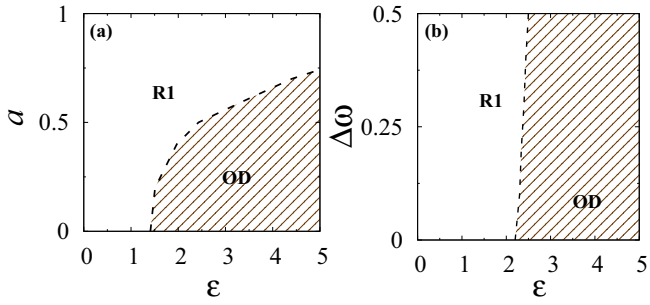

FIG. 16. (a) Two-parameter phase diagram of $N = 100$ globally coupled nonidentical Stuart-Landau oscillators in (ϵ, a) parameter space for $\Delta\omega = 0.3$, and (b) two-parameter phase diagram in $(\epsilon, \Delta\omega)$ parameter space for $a = 0.5$. The parameter space marked as R1 corresponds to the bistable region of two distinct quasiperiodic oscillatory states.

those observed for the case of two coupled Stuart-Landau oscillators, thereby corroborating the robustness and generic nature of the effect of the limiting factor.

VIII. SUMMARY AND CONCLUSIONS

We have considered two-coupled Stuart-Landau limit cycle oscillators by coupling x variables to the evolution equation among the dissimilar variables with a repulsive link and a simple limiting factor. We find that the limiting factor in the intrinsic variable that limits the interaction between the coupled oscillators indeed facilitates the manifestation of stable steady states from the stable oscillatory state. In contrast, the limiting factor in the intrinsic variable of the normal diffusive coupling is known to destabilize the stable steady states, thereby facilitating the manifestation of the stable oscillatory state [18]. In particular, the limiting factor in the intrinsic variable facilitates the onset of the nontrivial amplitude death among the coupled identical oscillators via the SNIPER bifurcation by destabilizing the in-phase oscillatory state. In contrast, the nontrivial amplitude death has been shown to emerge via a subcritical pitchfork bifurcation in general in the literature. Furthermore, the symmetry-breaking OD state manifests via a saddle-node bifurcation. The out-of-phase oscillatory state loses its stability via the homoclinic bifurcation. Only in-phase and out-of-phase oscillatory states coexist for large values of the limiting factor. Nevertheless, below a critical value of the limiting factor there is a transition from the in-phase oscillatory state to the nontrivial amplitude death (and oscillation death) state via the out-of-phase oscillatory state in a large range of the limiting factor. There are regions of bistability among the observed collective dynamical states. Decreasing values of the limiting factor facilitate the emergence of the nontrivial amplitude death state in a large range of the repulsive coupling strength. The dynamical transitions are investigated both as a function of the repulsive coupling strength and the natural frequency. We have deduced the evolution equation for the perturbations governing the stability of the observed dynamical states. We have also deduced the stability conditions for the SNIPER and pitchfork bifurcations using linear stability analysis, which are found to agree well with the simulation boundaries using the XPPAUT software.

In the case of coupled nonidentical Stuart-Landau oscillators with frequency mismatch, there is a transition from quasiperiodic oscillation to the oscillation death state via periodic oscillations. The quasiperiodic oscillations QP1 and QP2 lose their stability via subsequent of torus bifurcations, resulting in periodic oscillations as a function of the coupling strength. The periodic oscillations Os1 and Os2 lose their stability via the SNIPER and homoclinic bifurcations, respectively, for further larger coupling strengths. The oscillation death state onsets via SNIPER bifurcation. The bifurcation curves corresponding to the nonidentical Stuart-Landau oscillators are obtained using the XPPAUT software and have also been verified numerically. The dynamical transitions are investigated both as a function of the repulsive coupling strength and the distribution of natural frequency. Thus, it is clearly evident that the limiting factor in the intrinsic variable that destabilizes the stable steady states facilitating the revival of oscillations in the normal diffusive coupling can also indeed lead to the counterintuitive effect of stabilizing the nontrivial steady state and oscillation death state via the SNIPER bifurcation, while the systems are repulsively coupled to the evolution equation of the dissimilar (conjugate) variables. The generic nature of the effect of the limiting factor in the employed coupling configuration is also validated using N coupled Stuart-Landau oscillators and two coupled FitzHugh-Nagumo oscillators. We strongly believe that the results of this manuscript will lead to further research activities in exploring the emergence of various other types of quenched states and their bifurcation transitions in several other complex systems in the presence of the limiting factor in the intrinsic variable, generalizing its versatile nature beyond its current limits.

ACKNOWLEDGMENTS

The work of V.K.C. is supported by the DST-CRG project under Grant No. CRG/2020/004353 and DST, New Delhi for computational facilities under the DST-FIST program (SR/FST/PS- 1/2020/135) in the Department of Physics. M.M. thanks the Department of Science and Technology, Government of India, for providing financial support through INSPIRE Fellowship No. DST/INSPIRE Fellowship/2019/IF190871. D.V.S. is supported by the DST-SERB-CRG Project under Grant No. CRG/2021/000816. W.Z. acknowledges support from the National Natural Science Foundation of China (NNSFC, Grant No. 12075089).

[1] A. Sharma and M. D. Shrimali, Amplitude death with mean field diffusion, Phys. Rev. E **85**, 057204 (2012).

[2] A. Prasad, M. Dhamala, B. M. Adhikari, and R. Ramaswamy, Amplitude death in nonlinear oscillators with nonlinear coupling, Phys. Rev. E **81**, 027201 (2010).

[3] T. Banerjee and D. Ghosh, Transition from amplitude to oscillation death under mean-field diffusive coupling, Phys. Rev. E **89**, 052912 (2014).

[4] N. K. Kamal, P. R. Sharma, and M. D. Shrimali, Oscillation suppression in indirectly coupled limit cycle oscillators, Phys. Rev. E **92**, 022928 (2015).

[5] A. Sharma, P. R. Sharma, and M. D. Shrimali, Amplitude death in nonlinear oscillators with indirect coupling, Phys. Lett. A **376**, 1562 (2012).

[6] A. Prasad, Amplitude death in coupled chaotic oscillators. Phys. Rev. E **72**, 056204 (2005).

[7] I. Z. Kiss and J. L. Hudson, Phase synchronization and suppression of chaos through intermittency in forcing of an electrochemical oscillator, Phys. Rev. E **64**, 046215 (2001).

[8] G. B. Ermentrout and N. Kopell, Oscillator death in systems of coupled neural oscillators, SIAM J. Appl. Math. **50**, 125 (1990).

[9] B. Gallego and P. Cessi, Decadal variability of two oceans and an atmosphere, J. Clim. **14**, 2815 (2001).
[10] P. Kumar, A. Prasad, and R. Ghosh, Stable phase-locking of an external-cavity diode laser subjected to external optical injection, J. Phys. B: At. Mol. Opt. Phys. **41**, 135402 (2008).
[11] K. Kumar, D. Biswas, T. Banerjee, W. Zou, J. Kurths, and D. V. Senthilkumar, Revival and death of oscillation under mean-field coupling: Interplay of intrinsic and extrinsic filtering, Phys. Rev. E **100**, 052212 (2019).
[12] W. Zou, D. V. Senthilkumar, M. Zhan, and J. Kurths, Quenching, aging, and reviving in coupled dynamical networks, Phys. Rep. **931**, 1 (2021).
[13] D. Ghosh, T. Banerjee, and J. Kurths, Revival of oscillation from mean-field-induced death: Theory and experiment, Phys. Rev. E **92**, 052908 (2015).
[14] D. Ghosh and T. Banerjee, Transitions among the diverse oscillation quenching states induced by the interplay of direct and indirect coupling, Phys. Rev. E **90**, 062908 (2014).
[15] L. Illing, Amplitude death of identical oscillators in networks with direct coupling, Phys. Rev. E **94**, 022215 (2016).
[16] W. Zou, C. G. Yao, and M. Zhan, Eliminating delay-induced oscillation death by gradient coupling, Phys. Rev. E **82**, 056203 (2010).
[17] W. Zou, D. V. Senthilkumar, M. Zhan, and J. Kurths, Reviving Oscillations in Coupled Nonlinear Oscillators, Phys. Rev. Lett. **111**, 014101 (2013).
[18] W. Zou, D. V. Senthilkumar, R. Nagao, Z. Kiss, Y. Tang, A. Koseska, J. Duan, and J. Kurths, Restoration of rhythmicity in diffusively coupled dynamical networks, Nat. Commun. **6**, 7709 (2015).
[19] W. Zou, M. Zhan, and J. Kurths, Revoking amplitude and oscillation deaths by low-pass filter in coupled oscillators, Phys. Rev. E **95**, 062206 (2017).
[20] P. R. Sharma, N. K. Kamal, U. K. Verma, K. Suresh, K. Thamilmaran, and M. D. Shrimali, Suppression and revival of oscillation in indirectly coupled limit cycle oscillators, Phys. Lett. A **380**, 3178 (2016).
[21] S. Majhi, B. K. Bera, S. K. Bhowmick, and D. Ghosh, Restoration of oscillation in network of oscillators in presence of direct and indirect interactions, Phys. Lett. A **380**, 3617 (2016).
[22] R. Nagao, W. Zou, J. Kurths, and I. Z. Kiss, Restoring oscillatory behavior from amplitude death with anti-phase synchronization patterns in networks of electrochemical oscillations, Chaos **26**, 094808 (2016).
[23] I. Tiwari, R. Phogat, A. Biswas, and P. Parmananda, Quenching of oscillations in a liquid metal via attenuated coupling, Phys. Rev. E **105**, L032201 (2022).
[24] B. Ermentrout, *Simulating, Analyzing, and Animating Dynamical Systems: A Guide to XPPAUT for Researchers and Students* (Society for Industrial & Applied Math (SIAM), Philadelphia, PA, 2002).
[25] R. Grimshaw, *Nonlinear Ordinary Differential Equations* (CRC Press, Boca Raton, FL, 2000).
[26] S. Bhandary, T. Kaur, T. Banerjee, and P. S. Dutta, Network resilience of FitzHugh-Nagumo neurons in the presence of nonequilibrium dynamics, Phys. Rev. E **103**, 022314 (2021).